Oil Shale, 2026, 43, 3, 261–279 https://doi.org/10.3176/oil.2026.3.02

# Characteristics and facies classification of oil shales in major continental basins of China

Hongbiao Wang[a,b], Duoxiao Sun[a,b], Hongliang Dang[a,b,c], Yanwei Bi[a,b], Pingchang Sun[a,b]*

[a] College of Earth Sciences, Jilin University, Changchun, Jilin 130061, China
[b] Key-Lab for Oil Shale and Paragenetic Minerals of Jilin Province, Changchun, Jilin 130061, China
[c] Qinghai Geological Survey, Xining 810000, China

Received 16 December 2025, accepted 1 July 2026, available online 3 August 2026

***Abstract.*** *The continental oil shales of China exhibit pronounced heterogeneity in organic matter abundance, mineral composition, and sedimentary structures. Characterizing their lithofacies is therefore fundamental for reconstructing depositional environments, assessing resource potential, and guiding resource development. In this study, oil shale data from major continental basins, including the Songliao, Ordos, and Junggar basins, were compiled, with a focus on TOC, XRD-derived mineralogical compositions, and sedimentary structural information. Based on an integrated evaluation of organic geochemical and sedimentological parameters, TOC, bedding characteristics, and mineralogy were selected as key criteria for lithofacies classification. Accordingly, continental oil shales in China were subdivided into 24 lithofacies types, such as organic-rich laminated argillaceous mudstone (RLAM) and organic-poor massive siliceous mudstone (PMSM). Among them, organic-rich laminated mixed mudstone (RLMM), organic-rich laminated siliceous mudstone (RLSM), and organic-rich laminated calcareous mudstone (RLCM) are identified as the most prospective lithofacies due to their relatively high TOC contents, favorable mineralogical brittleness, and well-developed lamination, which collectively indicate superior hydrocarbon generation potential and reservoir quality.*

***Keywords:*** *lithofacies classification, oil shale, continental basin, total organic carbon, mineral composition.*

* Corresponding author, sunpingchang711@126.com

## 1. Introduction

Oil shale is a fine-grained sedimentary rock enriched in organic matter that can generate hydrocarbons upon heating [1]. As one of the most promising unconventional energy resources [2, 3], oil shale is characterized by abundant reserves, wide geographic distribution, and substantial potential for both direct utilization and in situ conversion technologies [4–6]. Lithofacies are defined as rocks or rock assemblages formed under specific depositional environments, reflecting sedimentary processes and environmental conditions. Lithofacies analysis provides a fundamental basis for evaluating the enrichment of organic sedimentary deposits, hydrocarbon generation potential, and development feasibility [7–9]. Accordingly, establishing a lithofacies classification framework for oil shale is crucial for elucidating its depositional evolution and resource potential.

At present, oil shale is commonly regarded as an extremely organic-rich shale, and a systematic lithofacies classification scheme has not yet been established. Previous studies have primarily focused on oil shale type classification. For example, Goodarzi et al. [10] divided oil shale into coastal, shallow-water, and deep-water types, whereas Lin [11] classified the oil shale of the Qingshankou Formation in the Songliao Basin into horizontally laminated, massive, and bioclastic oil shale. Given that existing mudstone and shale classification schemes typically incorporate parameters such as mineral composition, organic matter abundance, organic matter type, sedimentary structures, and grain size [7, 12–14], these parameters provide a robust methodological foundation for oil shale lithofacies classification in this study.

Compared with marine oil shale, terrestrial oil shale in China exhibits pronounced heterogeneity, more complex material sources, and broader ranges of organic matter and mineral compositions [15]. Moreover, inconsistencies in classification criteria among different studies hinder reliable inter-basin comparisons. The establishment of a unified lithofacies classification scheme for oil shale can effectively address these limitations. In this study, datasets on the sedimentary structures, organic matter abundance indices, and mineral assemblages of oil shale from six representative basins in China (Songliao, Ordos, Junggar, Maoming, Fushun, and Qaidam) were systematically compiled. By comparatively analyzing the variations in these parameters among different basins, a lithofacies classification framework for oil shale in terrestrial basins of China is established.

## 2. Characteristics of oil shale

### 2.1. Formation ages of oil shales in representative basins

Oil shales in China's terrestrial basins were primarily deposited from the Mesozoic to the Cenozoic, developing across diverse tectonic settings,

including rift basins, foreland basins, and cratonic basins, with deposition predominantly occurring in deep- to semi-deep lacustrine environments [16] (Table 1). Six representative basin oil shales were selected for this study. The Maoming and Fushun basins are small Cenozoic basins controlled by major faults, yet they host abundant oil shale resources within relatively limited areas [16, 17]. The Qingshankou Formation oil shale in the Upper Cretaceous of the Songliao Basin formed during the post-rift thermal subsidence stage [11, 18]. In the Qaidam Basin, the Shimengou Formation oil-bearing shale sequences were deposited in the late Middle Jurassic, representing a transitional phase from rifting to thermal subsidence [19]. In contrast, the Ordos Basin, a stable cratonic basin, contains oil shale in the Upper Triassic Yanchang Formation, reflecting a deep-lake depositional system developed under long-term basin stability [16]. The Lucaogou Formation oil shale in the Permian of the Junggar Basin was deposited in a terrestrial foreland basin during the molasse stage, influenced by the amalgamation of the Junggar and Tarim blocks [16]. Despite spanning a wide temporal range, these oil shales share common environmental characteristics, including rapid lake-basin subsidence, a warm and humid climate, and high lacustrine productivity, which collectively provided favorable conditions for the preservation and accumulation of abundant organic matter.

**Table 1.** Formation ages and depositional characteristics of oil shales in representative basins in China

| Basin | Type | Representative stratigraphic unit | Formation age | Depositional environment | References |
|---|---|---|---|---|---|
| Maoming | Rift basin | Youganwo Fm | Paleogene | Semi-deep lake | [17] |
| Fushun | Strike-slip basin | Jijuntun Fm | Paleocene–Eocene | Semi-deep to deep lake | [16] |
| Songliao | Rift basin | Qingshankou Fm | Upper Cretaceous | Deep lake | [11, 18] |
| Qaidam | Rift basin | Shimengou Fm | Middle–Late Jurassic | Semi-deep to deep lake | [19] |
| Ordos | Cratonic basin | Yanchang Fm | Upper Triassic | Semi-deep to deep lake | [16] |
| Junggar | Foreland basin | Lucaogou Fm | Middle Permian | Semi-deep to deep lake | [16] |

## 2.2. Sedimentary structure characteristics

A comparative analysis of sedimentary structures in oil shales from six basins reveals that China's terrestrial basin oil shales predominantly develop three structural types: laminated → bedded → massive (Fig. 1), reflecting variations in water-body stability, hydrodynamic intensity, sedimentation rate, and sediment composition. Laminated structures are particularly characteristic of deep- to semi-deep lake deposits. The upper oil shales of the Songliao, Fushun, Maoming, and Qaidam basins exhibit well-developed fine laminations (Fig. 1a, d, g, i), indicative of strong water stratification, low physical disturbance, and minimal sediment dilution [11, 16, 17, 19]. In contrast, bedded or massive structures are more frequently observed in the Ordos and Junggar basins at lake-margin locations or during periods of enhanced sediment supply,

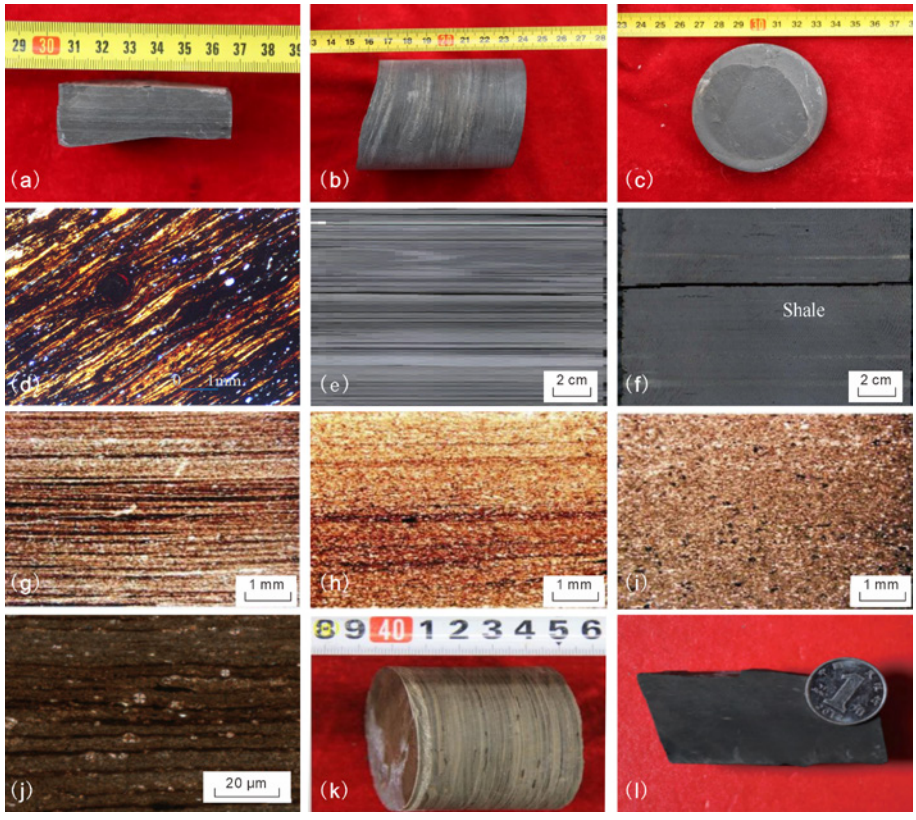


**Fig. 1.** Core samples and photomicrographs of oil shales [11, 18–21]. (a–c) Qingshankou Formation, Songliao Basin: oil shales displaying laminated, bedded, and massive structures, respectively; (d–f) Yanchang Formation, Ordos Basin: oil shales displaying laminated, bedded, and massive structures, respectively; (g–i) Lucaogou Formation, Junggar Basin: oil shales displaying laminated, bedded, and massive structures, respectively; (j–l) Shimengou Formation, Qaidam Basin: oil shales displaying laminated, bedded, and massive structures, respectively.

reflecting higher sedimentation rates, increased lake disturbances, and greater clastic input [20, 21]. Overall, laminated structures represent the most prevalent and defining sedimentary feature of high-quality terrestrial oil shales in China. They control rock brittleness, pore structure, and the distribution of organic matter, and their degree of development largely determines lithofacies assemblages and the potential exploitability of oil shale.

### 2.3. Organic matter abundance and type

Total organic carbon (TOC) of oil shales from six terrestrial basins in China generally falls within a medium- to high range (approximately 5–25%), although significant differences exist among depositional systems (Fig. 2).

Geochemical data indicate that the TOC content of the Youganwo Formation oil shales in the Maoming Basin ranges from 3.7% to 28.9%, with a mean of 13.4%. The hydrogen index (HI) varies between 332 and 1108 mg HC/g TOC, averaging 721.8 mg HC/g TOC. Organic matter is predominantly type I kerogen.

For the Jijuntun Formation oil shales in the Fushun Basin, TOC ranges from 2.3% to 30.3%, with a mean of 10.3%, and HI ranges from 102 to 699 mg HC/g TOC, averaging 475.7 mg HC/g TOC (Fig. 2). The organic matter mainly comprises type I and type II kerogen.

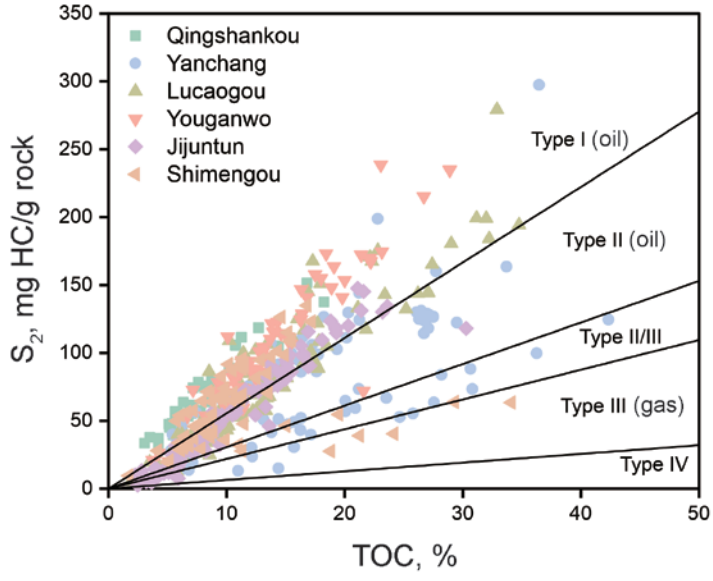


**Fig. 2.** TOC–$S_2$ cross plot for immature oil shales [48]. Qingshankou Formation data are from [49]; Yanchang Formation data are from [20, 22, 50–52]; Lucaogou Formation data are from [53]; Youganwo Formation data are from [54, 55]; Jijuntun Formation data are from [38]; Shimengou Formation data are from [56, 57].

The TOC content of the Qingshankou Formation oil shales in the Songliao Basin ranges from 4.3% to 18.3%, with an average of 7.8%. Laminated oil shales exhibit higher TOC (mean 11.3%) than bedded (5.9%) and massive (5.5%) counterparts. HI is relatively high, ranging from 362 to 1097 mg HC/g TOC, with a mean of 838.2 mg HC/g TOC (Fig. 2). Organic matter is primarily lacustrine in origin [11, 18], dominated by type I kerogen, with type II kerogen as a subordinate component.

In the Shimengou Formation of the Qaidam Basin, TOC mostly ranges from 4.2% to 29.3%, averaging 10.7%, except for a few samples with extremely high TOC (up to 34.1%). HI varies from 147 to 903 mg HC/g TOC, averaging 610.2 mg HC/g TOC. Organic matter is mainly type I and type II kerogen, with minor type III occurrences (Fig. 2).

The Yanchang Formation oil shales in the Ordos Basin display high TOC values ranging from 3.6% to 42.3%, with a mean of 19.2%. HI ranges from 103 to 871 mg HC/g TOC, averaging 437.6 mg HC/g TOC (Fig. 2). Organic matter is derived from a mixture of aquatic organisms and higher plants [22, 23], with the maceral composition dominated by vitrinite (up to 79.3%). Kerogen is predominantly type II, with minor type I.

The TOC content of the Lucaogou Formation oil shales in the Junggar Basin ranges from 3.2% to 34.8%, averaging 14.1%, with HI between 215 and 1068 mg HC/g TOC (mean 574.1 mg HC/g TOC) (Fig. 2). Organic matter is mainly lamalginite, with minor contributions from higher plant debris [21], comprising type I and type II kerogen.

Large terrestrial basins such as the Ordos and Junggar basins are generally rich in organic matter, often exceeding 10% and locally surpassing 20–30%, reflecting high productivity and good preservation in deep-lake environments. In smaller Cenozoic basins such as the Maoming and Fushun basins, strong basin confinement and rapid sedimentation allow the formation of organic-rich oil shales with a TOC content of 10–20%. Overall, China's terrestrial oil shales are dominated by type I algal- and bacterial-derived kerogen, with minor contributions of type II and type III kerogen from terrestrial higher plants at basin margins.

### 2.4. Mineral composition characteristics

The mineral composition of terrestrial oil shales in China exhibits clear variations related to depositional environments, but overall can be summarized as combinations of three main groups: clay minerals, siliceous minerals, and carbonate minerals [9, 14] (Fig. 3). The Songliao, Junggar, and Ordos basins received relatively strong terrigenous clastic input, resulting in generally higher quartz and feldspar contents (quartz up to 25–40%). In contrast, the Maoming and Fushun basins, characterized by strongly confined lakes and limited external input, contain higher clay mineral contents (50–75%) and relatively low quartz content. The Qaidam Basin exhibits a transition from

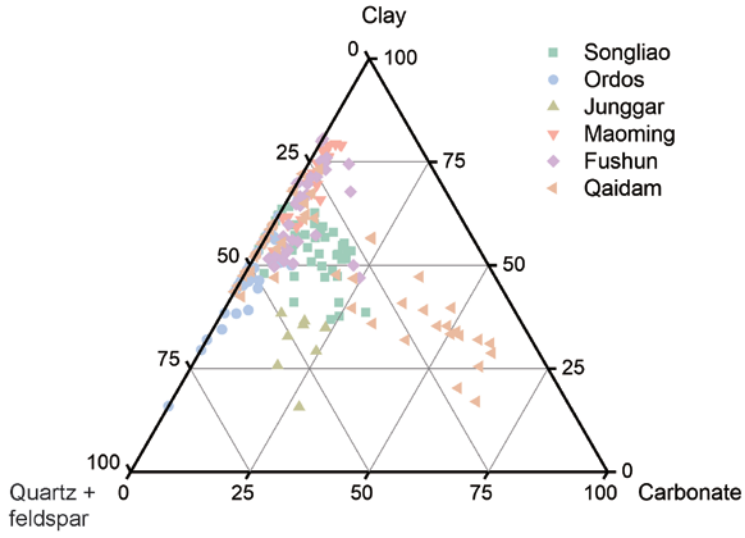


**Fig. 3.** Ternary diagram of mineral composition in oil shales. Songliao Basin data are from [11, 18]; Ordos Basin data are from [22, 40]; Junggar Basin data are from [58]; Maoming Basin data are from [17]; Fushun Basin data are from [38, 39]; Qaidam Basin data are from [19, 56, 57, 59, 60].

terrigenous-dominated to mixed terrigenous and autochthonous deposition (25–35%) [19].

Specifically, in the Maoming Basin, clay minerals dominate the mineral composition, ranging from 48% to 75%, with a mean of 64.9%. Siliceous minerals are relatively low, with quartz ranging from 12% to 37% (mean 22.7%) and feldspar from 0% to 4% (mean 1.9%).

For the Jijuntun Formation oil shales in the Fushun Basin, clay minerals are the most abundant (44.3–79%, mean 58.1%), followed by quartz (12–39%, mean 26.2%), with minor amounts of feldspar, calcite, and pyrite.

In the Qingshankou Formation of the Songliao Basin, siliceous minerals range from 27.0% to 47.9%, with a mean of 34.5%. Carbonate minerals are generally low, averaging around 11.1%. Some bedded and massive oil shale samples contain bioclasts such as foraminifera, which locally increase carbonate content.

In the Shimengou Formation of the Qaidam Basin, the mineral assemblage of oil shales is dominated by clay minerals, quartz, and calcite, with mean contents of 45.5%, 15.5%, and 30.4%, respectively. Mineral composition varies with oil shale quality. Lower Shimengou Formation oil shales, characterized by lower TOC content, are dominated by quartz (average 38.5%) and clay minerals (average 56.3%), whereas in the upper formation, laminated oil shales

are highly developed, the carbonate content increases significantly (average 30.7%) while quartz decreases (average 14.5%), resulting in an assemblage dominated by carbonate and clay minerals.

In the Yanchang Formation of the Ordos Basin, terrigenous clastic minerals are abundant, with quartz averaging 28.7% and plagioclase averaging 12.9%. Carbonate minerals are low, averaging 1.9%, while clay minerals range from 20% to 64.7%, averaging 45.8%. Additionally, pyrite is present, reaching up to 19.3%.

In the Lucaogou Formation of the Junggar Basin, oil shale minerals are mainly siliceous and carbonate clastic minerals, with lower clay content. Quartz averages 32.7%, feldspar 15.5%, carbonate minerals 19.5%, and clay minerals 30.6%.

## 3. Discussion

### 3.1. Parameters for oil shale facies classification

Previous research [24, 25] has systematically summarized the criteria for classifying mudstone facies, identifying color, mineral composition and abundance, biological components, primary sedimentary structures, compaction and deformation features, and diagenetic structures as key parameters. Together, these constitute a multi-proxy framework for facies classification. A well-defined facies classification system is vital for understanding sedimentary processes and depositional environments and serves as an essential reference for sedimentary resource evaluation and shale oil and gas exploration [12]. Facies schemes and nomenclature should simultaneously fulfill the functions of "description," "assessment," and "prediction" [14]. Specifically, they should describe physical, chemical, and biological variations at scales ranging from micrometers to meters, assess primary depositional processes and mechanisms, and predict post-depositional diagenetic pathways and the evolution of overall rock properties. However, time-variant features, such as color, are unsuitable as classification parameters [14].

Considering organic geochemical data, sedimentary structures, and mineral assemblages from major oil shale basins in China, and referencing previous shale facies classification schemes [7–9], this study classifies Chinese oil shale facies using three independent criteria: organic matter abundance, sedimentary structure, and mineral composition (Fig. 4). These parameters comprehensively capture the physical and chemical characteristics of the shales, reflect depositional processes and mechanisms, and provide insight into provenance, depositional environments, and predictive diagenetic evolution.

Organic matter abundance reflects paleo-lake productivity, sedimentation rates, and redox conditions [26–28]. TOC, as the principal indicator of organic matter abundance, is a key parameter for evaluating the hydrocarbon generation potential of oil shales. Variations in TOC directly control the

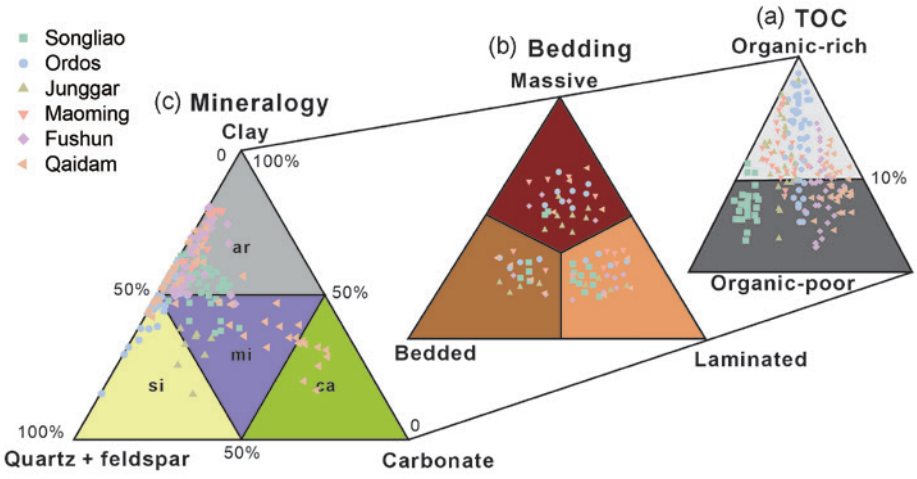


**Fig. 4.** Facies of oil shales are classified using a three-parameter scheme encompassing TOC content (a), bedding type (b), and mineralogy (c). Abbreviations: ar – argillaceous mudstone, mi – mixed mudstone, si – siliceous mudstone, ca – calcareous mudstone.

hydrocarbon-generating capacity of the rocks. Compared with existing TOC evaluation standards for mudstones [8], oil shales, being highly organic-rich, generally exhibit elevated TOC values. Moreover, as immature source rocks, oil shales require thermal input for efficient hydrocarbon extraction, necessitating stricter criteria in potential assessments. In China's continental basins, most oil shales display TOC values ranging from 5.8% to 24.1%, and a threshold of 10% is adopted here to distinguish between organic-rich and organic-poor shales. The TOC threshold of 10% corresponds approximately to the median–upper range of the dataset (5.8–24.1%), representing relatively organic-rich oil shale. This cutoff is also consistent with commonly adopted evaluation criteria for high-quality oil shale in previous studies.

Sedimentary structures in oil shales record abundant geological information and are essential for interpreting depositional history, resource exploration, and paleoenvironmental evolution. Laminae – defined as the smallest indivisible units of bedding with thicknesses less than 1 cm – represent the fundamental structural element [29]. Although no universally accepted theory exists for the origin of fine-grained sediment laminae [30–33], their geometry, continuity, and pattern are widely used in lithological descriptions and provide preliminary insights into primary depositional processes and mechanisms. Compared with general fine-grained sediments [34], oil shales exhibit more stable deposition, with straighter, more continuous laminae. Following previous studies [8, 35], this work quantitatively classifies sedimentary structures into three types according to lamina development: laminated (< 1 mm), bedded (1 mm–1 cm), and massive (laminae absent).

Variations in mineral composition not only reflect basin provenance, paleoclimate, and lake chemistry but also influence porosity, brittleness, and potential for exploitation [14, 34]. Minerals are categorized into three major components: siliceous, carbonate, and clay minerals. Differences in mineral assemblages affect the mechanical properties of the strata and the adsorption capacity of organic matter [36]. Using a 50% content threshold (Fig. 4c), lithology is classified into four types: argillaceous mudstone, mixed mudstone, siliceous mudstone, and calcareous mudstone.

As illustrated in Figure 4, a comprehensive classification scheme based on organic matter abundance, sedimentary structure, and mineral composition allows theoretical subdivision of oil shales in China's continental basins into 24 facies types (Table 2). In practice, however, only one to a few dominant facies typically develop in each basin. Notably, for the same stratigraphic interval, variations in burial depth and organic matter maturity across different basin regions result in significant differences in clay content and TOC, and variations in sample collection depth among studies can further affect facies determination. Therefore, this study primarily relies on data from shallowly buried, thermally immature oil shales as the basis for facies classification. The selection of predominantly shallow-buried, immature oil shale samples aims to preserve primary depositional and mineralogical characteristics, thereby minimizing thermal alteration effects and ensuring that lithofacies classification reflects original sedimentary and organic geochemical features.

**Table 2.** Facies types of oil shales in China's continental basins

| TOC | Bedding | Mineralogy | Lithofacies |
|---|---|---|---|
| Organic-rich | Laminated | Fig. 4a | Organic-rich laminated argillaceous mudstone (RLAM) |
| | | | Organic-rich laminated mixed mudstone (RLMM) |
| | | | Organic-rich laminated siliceous mudstone (RLSM) |
| | | | Organic-rich laminated calcareous mudstone (RLCM) |
| | Bedded | | Organic-rich bedded argillaceous mudstone (RBAM) |
| | | | Organic-rich bedded mixed mudstone (RBMM) |
| | | | Organic-rich bedded siliceous mudstone (RBSM) |
| | | | Organic-rich bedded calcareous mudstone (RBCM) |
| | Massive | | Organic-rich massive argillaceous mudstone (RMAM) |
| | | | Organic-rich massive mixed mudstone (RMMM) |
| | | | Organic-rich massive siliceous mudstone (RMSM) |
| | | | Organic-rich massive calcareous mudstone (RMCM) |

*Continued on the next page*

**Table 2.** *continued*

| TOC | Bedding | Mineralogy | Lithofacies |
|---|---|---|---|
| Organic-poor | Laminated | Fig. 4a | Organic-poor laminated argillaceous mudstone (PLAM) |
| | | | Organic-poor laminated mixed mudstone (PLMM) |
| | | | Organic-poor laminated siliceous mudstone (PLSM) |
| | | | Organic-poor laminated calcareous mudstone (PLCM) |
| | Bedded | | Organic-poor bedded argillaceous mudstone (PBAM) |
| | | | Organic-poor bedded mixed mudstone (PBMM) |
| | | | Organic-poor bedded siliceous mudstone (PBSM) |
| | | | Organic-poor bedded calcareous mudstone (PBCM) |
| | Massive | | Organic-poor massive argillaceous mudstone (PMAM) |
| | | | Organic-poor massive mixed mudstone (PMMM) |
| | | | Organic-poor massive siliceous mudstone (PMSM) |
| | | | Organic-poor massive calcareous mudstone (PMCM) |

### 3.2. Oil shale facies classification

Facies variations in China's lacustrine basins reflect the combined influences of paleoclimate, basin type, water column stratification, sediment supply, and lake productivity [37]. The Songliao, Fushun, and Maoming basins are predominantly characterized by laminated argillaceous mudstone facies, indicating stable water column stratification and minimal hydrodynamic disturbance during deposition [11, 17, 18, 38, 39]. In contrast, the Ordos and Junggar basins are dominated by organic-rich mixed mudstone and organic-rich siliceous mudstone facies, with elevated carbonate and siliceous mineral contents, high lake productivity, and abundant terrigenous and autochthonous sediment supply [21, 22, 40]. The Shimengou Formation in the Qaidam Basin corresponds to a Middle Jurassic transitional paleoclimate, shifting from humid to arid conditions, which influenced lake productivity, organic matter preservation, and sediment supply, thereby shaping the facies assemblage of the Shimengou oil shales [19].

Within individual basins, facies assemblages follow discernible patterns. The Qingshankou Formation in the Songliao Basin develops organic-rich laminated argillaceous mudstone (RLAM), organic-rich bedded argillaceous mudstone (RBAM), organic-rich laminated mixed mudstone (RLMM), organic-poor laminated argillaceous mudstone (PLAM), organic-poor bedded

argillaceous mudstone (PBAM), organic-poor massive argillaceous mudstone (PMAM), organic-poor laminated mixed mudstone (PLMM), organic-poor bedded mixed mudstone (PBMM), and organic-poor massive mixed mudstone (PMMM) facies. In the Ordos Basin, facies include RLAM, organic-rich laminated siliceous mudstone (RLSM), RBAM, organic-rich bedded siliceous mudstone (RBSM), organic-rich massive argillaceous mudstone (RMAM), organic-rich massive siliceous mudstone (RMSM), and organic-poor massive siliceous mudstone (PMSM). The Permian oil shales of the Junggar Basin display a broader diversity, including RLSM, RLMM, RBSM, organic-rich bedded mixed mudstone (RBMM), RMSM, organic-rich massive mixed mudstone (RMMM), organic-poor laminated siliceous mudstone (PLSM), PLMM, organic-poor bedded siliceous mudstone (PBSM), PBMM, PMSM, and PMMM. The Fushun and Maoming basins show similar assemblages, with RLAM, RBAM, RMAM, PLAM, PBAM, and PMAM facies. The Qaidam Basin exhibits the highest facies diversity, encompassing nearly all oil shale types, with RLAM, organic-rich laminated calcareous mudstone (RLCM), RLMM, PBSM, PBAM, PMSM, and PMAM being particularly common.

### 3.3. Implications of facies for hydrocarbon generation and resource assessment

Facies serve as a critical link connecting depositional processes, organic matter accumulation, and the hydrocarbon generation potential of lacustrine oil shales [41]. Variations in facies not only reflect differences in depositional environments and organic matter input but also govern the hydrocarbon generation, expulsion, and in-situ transformation potential of oil shale sequences [42]. Essentially, each facies represents a distinct “organic matter–mineral–porosity” system [42].

Identifying organic-rich facies with well-developed lamination and high brittleness indices is particularly critical for assessing hydrocarbon potential and producibility. Laminated facies, which form under low depositional rates, typically exhibit elevated TOC values [41] and favor the development of interlayer microfractures [43]. Rigid components, including siliceous and carbonate minerals, enhance compaction resistance, thereby promoting the formation and preservation of intergranular porosity [44], whereas clay minerals are generally inversely correlated with porosity development. During in-situ transformation, organic acids released from the thermal maturation of organic matter can dissolve carbonate and feldspar minerals [45], further improving reservoir properties.

The brittleness index (BI) is defined as the weight fraction of siliceous plus carbonate minerals relative to the total mineral content (siliceous + carbonate + clay minerals) [46]. Rocks with BI > 60% exhibit brittle behavior, whereas those with BI < 60% display ductility [36, 47]. Consequently, organic-rich laminated facies with high BI constitute the most promising oil shale targets.

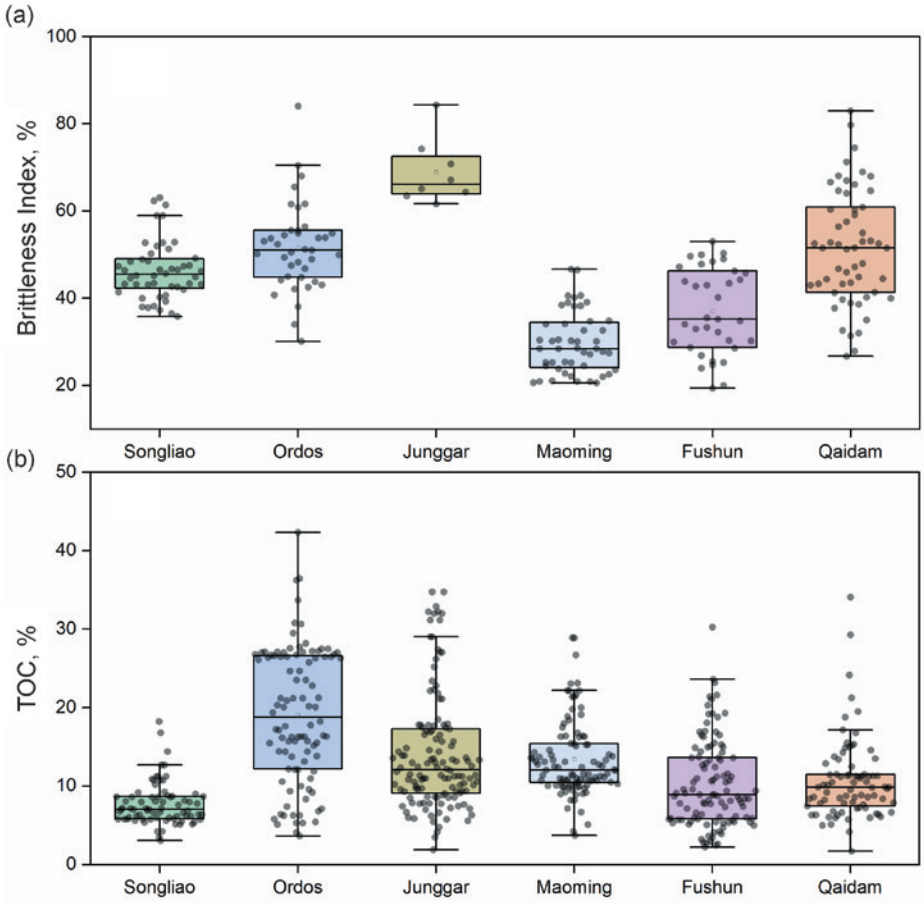


**Fig. 5.** Distribution of brittleness index (a) and TOC content (b) for oil shales from different basins. The upper and lower boundaries of the boxes represent the 75th and 25th percentiles, respectively.

At the facies scale, RLMM, RLSM, and RLCM represent the most favorable "sweet spots" within basins. At the basin scale, the Junggar Basin stands out with the highest brittle mineral content (BI = 68.9%) and relatively high TOC content (average 14.14%) (Fig. 5). Furthermore, the Lucaogou Formation oil shales in the Junggar Basin are hydrogen-rich, with HI values reaching 574.1 mg/g TOC, marking it as the basin with the greatest oil shale exploitation potential.

## 4. Conclusions

This study presents an oil shale facies classification scheme tailored for lacustrine basins in China, based on organic geochemical parameters, mineralogical composition, and depositional structures of oil shales from six major basins (Songliao, Ordos, Junggar, Maoming, Fushun, and Qaidam). Systematic basin-scale comparisons were also conducted. The main findings are summarized as follows:

1. By integrating three key parameters – TOC content, depositional structure, and mineralogical composition – 24 operationally practical lacustrine oil shale facies were delineated. This classification effectively captures geological processes such as paleo-productivity, depositional conditions, and sediment provenance, exhibiting strong applicability and comparability across different basins.
2. Analysis of the oil shale characteristics across these basins indicates that the organic-rich laminated mixed mudstone (RLMM), organic-rich laminated siliceous mudstone (RLSM), and organic-rich laminated calcareous mudstone (RLCM) facies represent the most favorable "sweet spots" for in-situ hydrocarbon generation. Basin-scale comparisons further highlight the Junggar Basin as possessing oil shales with the highest development potential.

## Data availability statement

The data that support the findings of this study are available from the corresponding author upon reasonable request.

## Acknowledgments

This work was supported by the Oil & Gas Major Project (grant No. 2025ZD1400803) and the National Natural Science Foundation of China (grant No. 42372125). The authors gratefully acknowledge the Editorial Board and the anonymous reviewers for their constructive comments, which have significantly improved the quality of this manuscript. We also thank Ms. Kadri Põdra for her assistance during the editorial process. The publication costs of this article were partially covered by the Estonian Academy of Publishers.

## References

1. Liu, Z.-J., Meng, Q.-T., Jia, J.-L. Key methods and technologies in the study of oil shale mineralization. *Journal of Palaeogeography*, 2019, **21**(1), 127–142.
2. Dyni, J. R. Geology and resources of some world oil-shale deposits. *Oil Shale*, 2003, **20**(3), 193–252. https://doi.org/10.3176/oil.2003.3.02

3. Na, J. G., Im, C. H., Chung, S. H., Lee, K. B. Effect of oil shale retorting temperature on shale oil yield and properties. *Fuel*, 2012, **95**, 131–135. https://doi.org/10.1016/j.fuel.2011.11.029
4. Yang, Q., Guo, W., Xu, S., Zhu, C. The autothermic pyrolysis in-situ conversion process for oil shale recovery: effect of gas injection parameters. *Energy*, 2023, **283**, 129134. https://doi.org/10.1016/j.energy.2023.129134
5. Wang, H., Niu, D., Luan, Z., Dang, H., Pan, X., Sun, P. Kinetic characteristics of secondary hydrocarbon generation from oil shale and coal at different maturation stages: insights from open-system pyrolysis. *International Journal of Coal Geology*, 2025, **308**, 104845. https://doi.org/10.1016/j.coal.2025.104845
6. Gavrilova, O., Vilu, R., Vallner, L. A life cycle environmental impact assessment of oil shale produced and consumed in Estonia. *Resources, Conservation and Recycling*, 2010, **55**(2), 232–245. https://doi.org/10.1016/j.resconrec.2010.09.013
7. Liu, B., Shi, J., Fu, X., Lyu, Y., Sun, X., Gong, L. et al. Petrological characteristics and shale oil enrichment of lacustrine fine-grained sedimentary system: a case study of organic-rich shale in first member of Cretaceous Qingshankou Formation in Gulong Sag, Songliao Basin, NE China. *Petroleum Exploration and Development*, 2018, **45**(5), 884–894. https://doi.org/10.1016/S1876-3804(18)30091-0
8. Wang, Y., Wang, X., Song, G., Liu, H., Zhu, D., Zhu, D. et al. Genetic connection between mud shale lithofacies and shale oil enrichment in Jiyang Depression, Bohai Bay Basin. *Petroleum Exploration and Development*, 2016, **43**(5), 759–768. https://doi.org/10.1016/S1876-3804(16)30091-X
9. Liu, Z., Liu, G., Hu, Z., Feng, D., Zhu, T., Bian, R. et al. Lithofacies types and assemblage features of continental shale strata and their implications for shale gas exploration: a case study of the Middle and Lower Jurassic strata in the Sichuan Basin. *Natural Gas Industry B*, 2020, **7**(4), 358–369. https://doi.org/10.1016/j.ngib.2019.12.004
10. Goodarzi, F., Gentzis, T., Sanei, H., Pedersen, P. K. Elemental composition and organic petrology of a Lower Carboniferous-age freshwater oil shale in Nova Scotia, Canada. *ACS Omega*, 2019, **4**(24), 20773–20786. https://doi.org/10.1021/acsomega.9b03227
11. Shen, L. *Characteristics and Prediction of Deep Oil Shale in the Upper Cretaceous Qingshankou Formation in the Southern Songliao Basin*. Master's thesis. Jilin University, China, 2020.
12. Liu, B., Wang, H., Fu, X., Bai, Y., Bai, L., Jia, M. et al. Lithofacies and depositional setting of a highly prospective lacustrine shale oil succession from the Upper Cretaceous Qingshankou Formation in the Gulong sag, northern Songliao Basin, northeast China. *AAPG Bulletin*, 2019, **103**(2), 405–432. https://doi.org/10.1306/08031817416
13. Tang, X., Jiang, Z., Huang, H., Jiang, S., Yang, L., Xiong, F. et al. Lithofacies characteristics and its effect on gas storage of the Silurian Longmaxi marine shale in the southeast Sichuan Basin, China. *Journal of Natural Gas Science and Engineering*, 2016, **28**, 338–346. https://doi.org/10.1016/j.jngse.2015.12.026

14. Peng, J., Hu, Z., Feng, D. The classification scheme for fine-grained sedimentary rocks: a review and a new approach based on five inherent rock attributes. *Gondwana Research*, 2025, **145**, 107–141. https://doi.org/10.1016/j.gr.2025.04.014
15. Huang, C., Zhang, J., Hua, W., Yue, J., Lu, Y. Sedimentology and lithofacies of lacustrine shale: a case study from the Dongpu sag, Bohai Bay Basin, eastern China. *Journal of Natural Gas Science and Engineering*, 2018, **60**, 174–189. https://doi.org/10.1016/j.jngse.2018.10.014
16. Liu, Z., Liu, R., Sun, P., Meng, Q., Hu, F. Oil shale characteristics and distribution in typical basins of China. *Journal of Jilin University (Earth Science Edition)*, 2020, **50**(2), 313–325. https://doi.org/10.13278/j.cnki.jjuese.20200017
17. Xu, C. *Geochemical Characteristics of Oil Shale in Youganwo Formation and its Aggregation Factors of Organic Matter, Maoming Basin*. Master's thesis. Jilin University, China, 2018.
18. Zhang, S. *Characteristics and Difference Analysis of Oil Shale in the First Member of Qingshankou Formation of Upper Cretaceous in Songliao Basin*. Master's thesis. Jilin University, China, 2021.
19. Xie, W. *Late Middle Jurassic Paleoclimate and Paleoenvironmental Evolution and Organic Matter Accumulation Mechanism, Qaidam Basin*. PhD thesis. Central South University, China, 2023.
20. Yunlai, B., Yuhu, M. Geology of the Chang 7 Member oil shale of the Yanchang Formation of the Ordos Basin in central north China. *Petroleum Geoscience*, 2020, **26**(2), 355–371. https://doi.org/10.1144/petgeo2018-091
21. Gao, Y. *Organic Geochemical Characteristics and its Paleoenvironmental Significance of the Middle Permian Oil Shale in the Southern Junggar Basin*. Master's thesis. Heibei GEO University, China, 2016.
22. Li, D., Li, R., Zhu, Z., Wu, X., Cheng, J., Liu, F. et al. Origin of organic matter and paleo-sedimentary environment reconstruction of the Triassic oil shale in Tongchuan City, southern Ordos Basin (China). *Fuel*, 2017, **208**, 223–235. https://doi.org/10.1016/j.fuel.2017.07.008
23. Li, D., Li, R., Zhu, Z., Wu, X., Liu, F., Zhao, B. et al. Elemental characteristics and paleoenvironment reconstruction: a case study of the Triassic lacustrine Zhangjiatan oil shale, southern Ordos Basin, China. *Acta Geochimica*, 2018, **37**(1), 134–150. https://doi.org/10.1007/s11631-017-0193-z
24. Potter, P. E., Maynard, J. B., Depetris, P. J. *Mud and Mudstones: Introduction and Overview*. Springer, Berlin, Heidelberg, 2005. https://doi.org/10.1007/b138571
25. Potter, P. E., Maynard, J. B., Pryor, W. A. *Sedimentology of Shale*. Springer New York, New York, NY, 1980. https://doi.org/10.1007/978-1-4612-9981-3
26. Calvert, S. E., Pedersen, T. F. Geochemistry of recent oxic and anoxic marine sediments: implications for the geological record. *Marine Geology*, 1993, **113**(1–2), 67–88. https://doi.org/10.1016/0025-3227(93)90150-T
27. Tyson, R. V. Sedimentation rate, dilution, preservation and total organic carbon: some results of a modelling study. *Organic Geochemistry*, 2001, **32**(2), 333–339. https://doi.org/10.1016/S0146-6380(00)00161-3

28. Horsfield, B., Curry, D. J., Bohacs, K., Littke, R., Rullkötter, J., Schenk, H. J. et al. Organic geochemistry of freshwater and alkaline lacustrine sediments in the Green River Formation of the Washakie Basin, Wyoming, U.S.A. *Organic Geochemistry*, 1994, **22**(3–5), 415–440. https://doi.org/10.1016/0146-6380(94)90117-1
29. Campbell, C. V. Lamina, laminaset, bed and bedset. *Sedimentology*, 1967, **8**(1), 7–26. https://doi.org/10.1111/j.1365-3091.1967.tb01301.x
30. Schimmelmann, A., Lange, C. B., Schieber, J., Francus, P., Ojala, A. E. K., Zolitschka, B. Varves in marine sediments: a review. *Earth-Science Reviews*, 2016, **159**, 215–246. https://doi.org/10.1016/j.earscirev.2016.04.009
31. Schieber, J., Southard, J., Thaisen, K. Accretion of mudstone beds from migrating floccule ripples. *Science*, 2007, **318**(5857), 1760–1763. https://doi.org/10.1126/science.1147001
32. Schieber, J. Experimental testing of the transport-durability of shale lithics and its implications for interpreting the rock record. *Sedimentary Geology*, 2016, **331**, 162–169. https://doi.org/10.1016/j.sedgeo.2015.11.006
33. Shinn, E. A., Steinen, R. P., Dill, R. F., Major, R. Lime-mud layers in high-energy tidal channels: a record of hurricane deposition. *Geology*, 1993, **21**(7), 603–606. https://doi.org/10.1130/0091-7613(1993)021<0603:LMLIHE>2.3.CO;2
34. Lazar, O. R., Bohacs, K. M., Macquaker, J. H. S., Schieber, J., Demko, T. M. Capturing key attributes of fine-grained sedimentary rocks in outcrops, cores, and thin sections: nomenclature and description guidelines. *Journal of Sedimentary Research*, 2015, **85**(3), 230–246. https://doi.org/10.2110/jsr.2015.11
35. Dong, L., Li, Y., Wang, D., Liu, H., Song, G., Li, Z. et al. The classification and significance of fine-grained deposits of micro-laminae rich in unconventional oil and gas resources. *Frontiers of Earth Science*, 2022, **16**(3), 635–656. https://doi.org/10.1007/s11707-021-0955-0
36. Wang, G., Carr, T. R. Methodology of organic-rich shale lithofacies identification and prediction: a case study from Marcellus Shale in the Appalachian basin. *Computers & Geosciences*, 2012, **49**, 151–163. https://doi.org/10.1016/j.cageo.2012.07.011
37. Chen, Z., Li, X., Chen, H., Duan, Z., Qiu, Z., Zhou, X. et al. The characteristics of lithofacies and depositional model of fine-grained sedimentary rocks in the Ordos Basin, China. *Energies*, 2023, **16**(5), 2390. https://doi.org/10.3390/en16052390
38. Strobl, S. A. I., Sachsenhofer, R. F., Bechtel, A., Gratzer, R., Gross, D., Bokhari, S. N. H. et al. Depositional environment of oil shale within the Eocene Jijuntun Formation in the Fushun Basin (NE China). *Marine and Petroleum Geology*, 2014, **56**, 166–183. https://doi.org/10.1016/j.marpetgeo.2014.04.011
39. Wang, L., Lu, Y., Chen, G., Xue, L., Zhang, Z., Wang, S. et al. Greenhouse gas emissions during oil shale crushing and its main controlling factors: a contrast study of oil shale in Yaojie and Fushun areas, China. *ACS Omega*, 2024, **9**(15), 17491–17505. https://doi.org/10.1021/acsomega.4c00435
40. Li, S., Zhu, R.-K., Cui, J.-W., Luo, Z., Cui, J.-G., Liu, H. et al. The petrological characteristics and significance of organic-rich shale in the Chang 7 member

of the Yanchang Formation, south margin of the Ordos basin, central China. *Petroleum Science*, 2019, **16**(6), 1255–1269. https://doi.org/10.1007/s12182-019-00386-0

41. Sun, N., Chen, T., Gao, J., Zhong, J., Huo, Z., Qu, J. Lithofacies and reservoir characteristics of saline lacustrine fine-grained sedimentary rocks in the northern Dongpu Sag, Bohai Bay Basin: implications for shale oil exploration. *Journal of Asian Earth Sciences*, 2023, **252**, 105686. https://doi.org/10.1016/j.jseaes.2023.105686
42. Liang, C., Wu, J., Cao, Y., Liu, K., Khan, D. Storage space development and hydrocarbon occurrence model controlled by lithofacies in the Eocene Jiyang Sub-basin, East China: significance for shale oil reservoir formation. *Journal of Petroleum Science and Engineering*, 2022, **215**, 110631. https://doi.org/10.1016/j.petrol.2022.110631
43. Xin, B., Zhao, X., Hao, F., Jin, F., Pu, X., Han, W. et al. Laminae characteristics of lacustrine shales from the Paleogene Kongdian Formation in the Cangdong Sag, Bohai Bay Basin, China: why do laminated shales have better reservoir physical properties? *International Journal of Coal Geology*, 2022, **260**, 104056. https://doi.org/10.1016/j.coal.2022.104056
44. Espitalie, J., Madec, M., Tissot, B. Role of mineral matrix in kerogen pyrolysis: influence on petroleum generation and migration. *AAPG Bulletin*, 1980, **64**(1), 59–66. https://doi.org/10.1306/2F918928-16CE-11D7-8645000102C1865D
45. Surdam, R. C., Crossey, L. J., Hagen, E. S., Heasler, H. P. Organic-inorganic interactions and sandstone diagenesis. *AAPG Bulletin*, 1989, **73**(1), 1–23. https://doi.org/10.1306/703C9AD7-1707-11D7-8645000102C1865D
46. Jin, X., Shah, S., Truax, J., Roegiers, J.-C. A practical petrophysical approach for brittleness prediction from porosity and sonic logging in shale reservoirs. In *SPE Annual Technical Conference and Exhibition*, October 2014, Amsterdam. SPE-170972-MS. https://doi.org/10.2118/170972-MS
47. Jarvie, D. M., Hill, R. J., Ruble, T. E., Pollastro, R. M. Unconventional shale-gas systems: the Mississippian Barnett Shale of north-central Texas as one model for thermogenic shale-gas assessment. *AAPG Bulletin*, 2007, **91**(4), 475–499. https://doi.org/10.1306/12190606068
48. Garry, P., Atta-Peters, D., Achaegakwo, C. Source-rock potential of the lower cretaceous sediments in SD - 1X well, offshore Tano Basin, south western Ghana. *Petroleum and Coal*, 2016, **58**(4), 476–489.
49. Feng, Z., Fang, W., Wang, X., Huang, C., Huo, Q., Zhang, J. et al. Microfossils and molecular records in oil shales of the Songliao Basin and implications for paleo-depositional environment. *Science in China Series D: Earth Sciences*, 2009, **52**(10), 1559–1571. https://doi.org/10.1007/s11430-009-0121-0
50. Chen, Y., Zhu, Z., Zhang, L. Control actions of sedimentary environments and sedimentation rates on lacustrine oil shale distribution, an example of the oil shale in the Upper Triassic Yanchang Formation, southeastern Ordos Basin (NW China). *Marine and Petroleum Geology*, 2019, **102**, 508–520. https://doi.org/10.1016/j.marpetgeo.2019.01.006

51. Gao, B., Wu, X., Zhang, Y., Chen, X., Bian, R., Li, Q. Hydrocarbon generation and evolution characteristics of Triassic Zhangjiatan oil shale in southern Ordos Basin. *Petroleum Geology & Experiment*, 2022, **44**(1), 24–32. https://doi.org/10.11781/sysydz202201024
52. Ma, W., Hou, L., Luo, X., Liu, J., Tao, S., Guan, P. et al. Generation and expulsion process of the Chang 7 oil shale in the Ordos Basin based on temperature-based semi-open pyrolysis: implications for in-situ conversion process. *Journal of Petroleum Science and Engineering*, 2020, **190**, 107035. https://doi.org/10.1016/j.petrol.2020.107035
53. Tao, S., Wang, Y., Tang, D., Wu, D., Xu, H., He, W. Organic petrology of Fukang Permian Lucaogou Formation oil shales at the northern foot of Bogda Mountain, Junggar Basin, China. *International Journal of Coal Geology*, 2012, **99**, 27–34. https://doi.org/10.1016/j.coal.2012.05.001
54. Xu, C., Hu, F., Meng, Q., Liu, Z., Shan, X., Zeng, W. et al. Organic matter accumulation in the Youganwo Formation (middle Eocene), Maoming Basin, South China: constraints from multiple geochemical proxies and organic petrology. *ACS Earth and Space Chemistry*, 2022, **6**(3), 714–732. https://doi.org/10.1021/acsearthspacechem.1c00383
55. Zhao, D.-F., Guo, Y.-H., Wang, G., Zhou, X.-Q., Zhou, Y.-Y., Zhang, J.-M. et al. Organic matter enrichment mechanism of Youganwo Formation oil shale in the Maoming Basin. *Heliyon*, 2023, **9**(2), e13173. https://doi.org/10.1016/j.heliyon.2023.e13173
56. Bai, Y.-Y., Xie, W.-Q., Liu, Z.-J., Xu, Y.-B. Formation and evolution mechanisms of coal and oil shale from the Middle Jurassic Shimengou Formation, northern Qaidam Basin, China. *Ore Geology Reviews*, 2022, **151**, 105206. https://doi.org/10.1016/j.oregeorev.2022.105206
57. Bai, Y., Liu, Z., George, S. C., Meng, J. A comparative study of different quality oil shales developed in the Middle Jurassic Shimengou Formation, Yuqia area, northern Qaidam Basin, China. *Energies*, 2022, **15**(3), 1231. https://doi.org/10.3390/en15031231
58. Pang, H., Pang, X., Dong, L., Zhao, X. Factors impacting on oil retention in lacustrine shale: Permian Lucaogou Formation in Jimusaer Depression, Junggar Basin. *Journal of Petroleum Science and Engineering*, 2018, **163**, 79–90. https://doi.org/10.1016/j.petrol.2017.12.080
59. Li, L., Liu, Z., George, S. C., Sun, P., Xu, Y., Meng, Q. et al. Lake evolution and its influence on the formation of oil shales in the Middle Jurassic Shimengou Formation in the Tuanyushan area, Qaidam Basin, NW China. *Geochemistry*, 2019, **79**(1), 162–177. https://doi.org/10.1016/j.geoch.2018.12.006
60. Guo, W., Chen, G., Li, Y., Li, Y., Zhang, Y., Zhou, J. et al. Factors controlling the lower radioactivity and its relation with higher organic matter content for middle Jurassic oil shale in Yuqia depression, northern Qaidam Basin, China: evidence from organic and inorganic geochemistry. *ACS Omega*, 2021, **6**(11), 7360–7373. https://doi.org/10.1021/acsomega.0c05618